



A SIMPLIFIED METHOD FOR CALCULATION OF LONG-TERM DEFLECTIONS IN COMPOSITE SLABS

A. Gholamhoseini¹, R.I. Gilbert² and M.A. Bradford³

ABSTRACT

Relatively little research has been reported on the time-dependent in-service behaviour of composite concrete slabs with profiled steel decking as permanent formwork and little guidance is available for calculating long-term deflections. The drying shrinkage profile through the thickness of a composite slab is greatly affected by the impermeable steel deck at the slab soffit, and this has only recently been quantified.

Based on an existing analytical model developed by the authors to calculate the time-dependent deflection of composite slabs, a simplified procedure, suitable for use in structural design, is proposed for calculating the time-dependent deflection of composite concrete slabs with steel decking as permanent formwork taking into account the time-dependent effects of creep and shrinkage. The method is illustrated by two examples and the results are compared with the laboratory measurements and with the values obtained from numerical analyses.

Introduction

Composite one-way concrete floor slabs with profiled steel decking as permanent formwork are commonly used in the construction of floors in buildings (Fig. 1). The steel decking supports the wet concrete of a cast-in-situ reinforced or post-tensioned concrete slab and, after the concrete sets, acts as external reinforcement. Embossments on the profiled sheeting provide the necessary shear connection to ensure composite action between the concrete slab and the steel decking.

Despite their common usage, relatively little research has been reported on the in-service behaviour of composite slabs. In particular, the drying shrinkage profile through the slab thickness (which is greatly affected by the impermeable steel decking) and the restraint to shrinkage provided by the decking have only recently been quantified (Gholamhoseini et al., 2012a,b; Gilbert et al., 2012; Ranzi et al. 2012, 2013). In their research, Gilbert et al. (2012) measured the non-linear variation of shrinkage strain through the thickness of several slab specimens, with and without steel decking at the soffit, and sealed on all exposed concrete surfaces except for the top surface. Carrier et al. (1975) measured the moisture contents of two bridge decks, one was a composite slab with profiled steel decking and the other was a conventional reinforced concrete slab permitted to dry from the top and bottom surfaces after the timber forms were removed. The moisture loss was significant only in the top 50 mm of the slab with profiled steel decking and in the top and bottom 50 mm of the conventionally reinforced slab regardless of the specimen size.

Gholamhoseini et al. (2012a,b) carried out an experimental study on the long-term behaviour of composite concrete slabs with two different types of steel decking (KF70 and KF40 manufactured by Fielders Australia) and subjected to sustained service loads and drying shrinkage. The results showed the dominant role played

¹Postdoctoral Research Fellow, Dept. of Civil and Natural Resources Engineering, University of Canterbury, Christchurch 8140, New Zealand (email: alireza.gholamhoseini@canterbury.ac.nz)

²Emeritus Professor, Centre for Infrastructure Engineering and Safety, The University of New South Wales, Kensington, NSW 2033, Australia

³Scientia Professor, Centre for Infrastructure Engineering and Safety, The University of New South Wales, Kensington, NSW 2033, Australia

by drying shrinkage in the long-term deflection of composite concrete slabs with steel decking as permanent formwork. Based on their findings, Gholamhoseini et al. (2012b) proposed a non-linear shrinkage profile through the thickness of a composite concrete slab, together with an analytical model based on the provisions of Australian Standard AS 3600-2009 for calculating the instantaneous and time-dependent curvature at a typical cross-section due to the effects of both load and non-linear shrinkage. They also proposed a shrinkage strain profile for concrete slabs on profiled steel decking that is suitable for use in structural design and a modification to the provisions of ACI 209.2R-08 for estimating the shrinkage strain and creep coefficient for deflection calculation in composite slabs (Gholamhoseini et al. (2014a)). Their proposals were developed empirically from experimental measurements of shrinkage-induced deflections and strain distributions in composite slabs.



Figure 1. Soffit of a one-way composite slab and beam floor system.

Notwithstanding the research mentioned above, there is still little design guidance available to practising engineers for predicting the in-service deformation of composite slabs. The techniques used to predict deflection and the on-set of cracking in conventionally reinforced concrete slabs are often applied inappropriately. Although techniques are available for the time-dependent analysis of composite slabs (Gilbert & Ranzi, 2011), due to lack of guidance in codes of practice, structural designers often specify the decking as sacrificial formwork, in lieu of timber formwork, and ignore the structural benefits afforded by the composite action. Of course this provides a conservative estimate of the ultimate strength of the slab and is quite unsustainable, but may well result in a significant under-estimation of deflection because of the shrinkage strain gradient and the restraint provided by the decking.

In this paper, an analytical model, previously proposed by the authors, has been used to generate simple-to-use graphs to obtain two parameters that are needed to calculate the creep and shrinkage-induced curvatures in a composite slab. Examples illustrating the use of the graphs are also presented and the results are compared with the values attained separately from experimental and analytical studies.

Time-Dependent Deflections

Shrinkage may cause significant changes in the distribution of internal strains with time in composite slabs. If the slab is not free to shorten (e.g. due to restraint caused by the steel decking), shrinkage produces internal tension in the concrete and, as this tension is eccentric to the centroid of the concrete cross-section, shrinkage-induced curvature results. Shrinkage-induced curvature at each cross-section along the span of a slab due to the restraint provided by the steel decking can lead to significant deflections. Creep of concrete also increases the curvature of the cross-section with time. The time-dependent deflection of a composite slab is also dependent on the development of time-dependent cracking and the reduction in tension stiffening with time, in addition to the increase in curvature at each cross-section due to creep of concrete, and the increase in curvature due to the restraint to concrete shrinkage provided by the steel decking.

Using the age-adjusted effective modulus method (AEMM), Gilbert (2001) derived empirical but simple-to-use equations to model the long-term creep and shrinkage-induced changes in curvature on reinforced concrete cross-sections under constant sustained internal actions. These equations account for the effects of cracking and the restraining action of the reinforcement. The equations for shrinkage-induced curvature (κ_{sh}) and creep-induced curvature (κ_{creep}) are as follows:

$$\kappa_{sh} = \frac{k_r \cdot \varepsilon_{sh}}{D} \quad (1)$$

$$\kappa_{creep} = \frac{\varphi(t, t_0)}{\alpha} \kappa_{i, sus} \quad (2)$$

where D is the overall depth of the cross-section; ε_{sh} is the shrinkage strain; $\varphi(t, t_0)$ is the creep coefficient at time t due to load first applied at age t_0 ; and $\kappa_{i,sus}$ is the instantaneous curvature due to the sustained load. The term α is a creep modification factor that accounts for the effects of cracking and the restraining action of the reinforcement on creep and is a function of the extent of cracking on the cross-section and the area and position of the bonded reinforcement in the tensile and compressive zones. For uncracked singly reinforced concrete cross-section, α ranges between 1.1 and 1.8, depending on the amount of reinforcement, while for cracked singly reinforced cross-sections, α ranges between 4.0 and 8.0. The term k_r is the shrinkage modification factor and depends on the extent of cracking, the level of tension stiffening and the area and position of bonded reinforcement in the tensile and compressive zones.

It should be emphasised that as creep and shrinkage occur simultaneously, it is in fact impossible to calculate the creep-induced deflection and the shrinkage-induced deflection separately. However, it can be reasonably assumed that the shrinkage-induced deflection of a slab is independent of load level (although it is affected to some extent by the level of cracking) and that the creep-induced deflection is roughly proportional to the level of loading. These assumptions justify the application of κ_{sh} and κ_{creep} to calculate creep and shrinkage-induced deflections separately.

As a basic assumption to derive the empirical equations, Gilbert (2001) assumed that the drying process takes place on both surfaces of the slab and that the shrinkage profile through the thickness of slab is uniform. Thus, the direct application of those equations in composite slabs without modification is inappropriate. When the load-induced and shrinkage-induced curvatures are calculated at selected sections along the span of a slab, the deflection may be obtained by double integration.

Analytical Modelling

An analytical procedure for the time-dependent analysis of composite concrete cross-sections with uniform shrinkage through the thickness of the concrete slab and with full interaction was presented by Gilbert and Ranzi (2011) using the age-adjusted effective modulus method (AEMM). Gilbert et al. (2012) extended the method to calculate the effects of a non-uniform shrinkage strain by layering the concrete cross-section, with the shrinkage strain specified in each concrete layer depending on its position within the cross-section and with the assumption of full shear interaction at service load levels.

Based on their experimental study, Gholamhoseini et al. (2012b) proposed a modification to the provisions of AS 3600-2009 to determine the shrinkage strain and creep coefficient for composite slabs. For a composite slab with profiled steel decking, if the average thickness of the concrete t_{ave} (in mm) is defined as the area of the concrete part of the cross-section A_c , divided by the width of the cross-section b , the hypothetical thickness used to account for the effect of the steel decking on the magnitude of creep coefficient and shrinkage strain is given by:

$$t_h = 50 + \frac{t_{ave}}{2} \text{ (in mm)} \quad (3)$$

With this value of t_h , the creep coefficient $\varphi(t, t_0)$ and shrinkage strain value $\varepsilon_{sh}(t, t_c)$ may be determined in accordance with AS 3600-2009. The measured shrinkage strain at any height y above the soffit of the composite slab with overall depth D , $\varepsilon_{sh}(y)$, may be approximated by Eq. (4):

$$\frac{\varepsilon_{sh}(y)}{\varepsilon_{sh}(t, t_c)} = \lambda + \gamma \left(\frac{y}{D} \right)^4 \quad (4)$$

where $\varepsilon_{sh}(0) = \lambda \varepsilon_{sh}(t, t_c)$ is the shrinkage strain at the bottom of the slab (at $y=0$) and $\varepsilon_{sh}(D) = (\lambda + \gamma) \varepsilon_{sh}(t, t_c)$ is the shrinkage strain at the top surface of the slab (at $y=D$). From the experimental results, $\lambda = 0.2$ provides a reasonable estimate, but γ appears to depend on the profile of the steel decking with proposed values of $\gamma = 0.5$ for the KF70 slabs (with 70 mm deep troughs) and $\gamma = 1.0$ for the KF40 slabs (with 40 mm deep troughs). For other decking profiles considered in that study, the ratio of trough height to slab thickness (r_d) was in the range 0.25 to 0.5. In this range, the following relationship for γ provides good agreement with the measured shrinkage profiles:

$$\gamma = 1.7 - 2.5r_d \quad (5)$$

Numerical Analysis

The age-adjusted effective modulus method (AEMM) was used in accordance with the model described previously by Gilbert et al. (2012) to calculate κ_{sh} and κ_{creep} for three slab thicknesses of $D = 135$ mm, $D = 150$ mm and $D = 180$ mm for each of two steel decking types KF70 and KF40 (from Fielders Australia and as shown in Fig. 2). For each decking type, two steel sheeting thicknesses were considered, namely $t_{sd} = 0.75$ mm and $t_{sd} = 1.0$ mm. The modulus of elasticity for the steel sheeting was $E_{sd} = 2 \times 10^5$ MPa. Analyses were undertaken for three different concrete strength, i.e. 25 MPa ($E_c = 26700$ MPa), 32 MPa ($E_c = 30100$ MPa), and 40 MPa ($E_c = 32800$ MPa). For each slab, both the cases of an uncracked section and a cracked section were considered.

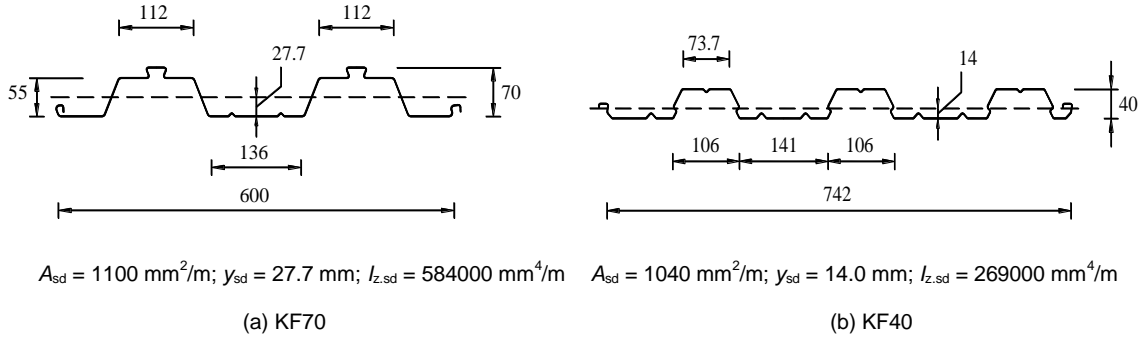


Figure 2. Dimensions (in mm) of each steel decking profile ($t_{sd} = 0.75$ mm).

From the calculated values of κ_{sh} and κ_{creep} , the values of k_r and α as defined in Eq. 1 and Eq. 2 were obtained. Figure 3 shows the variation in the values of k_r and α for 150-mm-thick and 180-mm-thick uncracked (UC) and cracked (CR) slabs with KF70 decking for varying compressive and tensile reinforcement ratios and varying concrete strengths. The complete set of values of k_r and α for uncracked and cracked slabs with different thicknesses and different decking types has been reported elsewhere (Gholamhoseini et al. 2014b). In the right hand side legend of each figure, the concrete strength is followed by the tensile reinforcement ratio $\rho = A_{sd} / bd$, where b is the width of the concrete compressive zone and d is the effective depth from the compressive edge to the centroid of the steel decking, i.e. $d = D - y_{sd}$. The horizontal axis of each figure is the compressive reinforcement ratio $\rho' = A_{sc} / bd'$, where A_{sc} is the area of any steel reinforcement in the compressive zone and d' is the distance from the tensile face (i.e. the soffit) of the slab to the centroid of the compressive reinforcement.

It is noted that the values for α for the uncracked slabs are in the range of 1.2 to 1.9 and, for the cracked slabs, α is in the range of 4.0 to 8.0. This is consistent with the ranges determined by Gilbert (2001) for uncracked and cracked cross-sections. It is well known that the increase of curvature with time due to creep of concrete is much greater on an uncracked cross-section, where the concrete over the entire cross-section is creeping, than on a cracked section, where only the concrete in the compressive zone is creeping. This phenomenon is discussed more thoroughly by Gilbert & Ranzi (2011).

Cracking of the tensile concrete in the slab is treated in the analysis here using the approach outlined in Eurocode 2, whereby the curvature after cracking is obtained from:

$$\kappa_{ave} = \zeta \kappa_{cr} + (1 - \zeta) \kappa_{uncr} \quad (6)$$

where κ_{cr} is the curvature at the section calculated by ignoring concrete in tension; κ_{uncr} is the curvature on the uncracked transformed section; and ζ is a distribution coefficient that accounts for the moment level and the degree of cracking and is given by:

$$\zeta = 1 - \beta \left(\frac{M_{cr}}{M_s} \right)^2 \quad \text{where } 0 \leq \zeta \leq 1.0 \quad (7)$$

The coefficient β accounts for the effects of duration of loading and is taken as 0.5 for sustained or long-

term loading. The cracking moment M_{cr} is the moment required to produce a maximum concrete tensile stress equal to the mean uniaxial tensile strength of concrete, f_{ctm} , and M_s^* is the maximum in-service moment on the section under consideration.

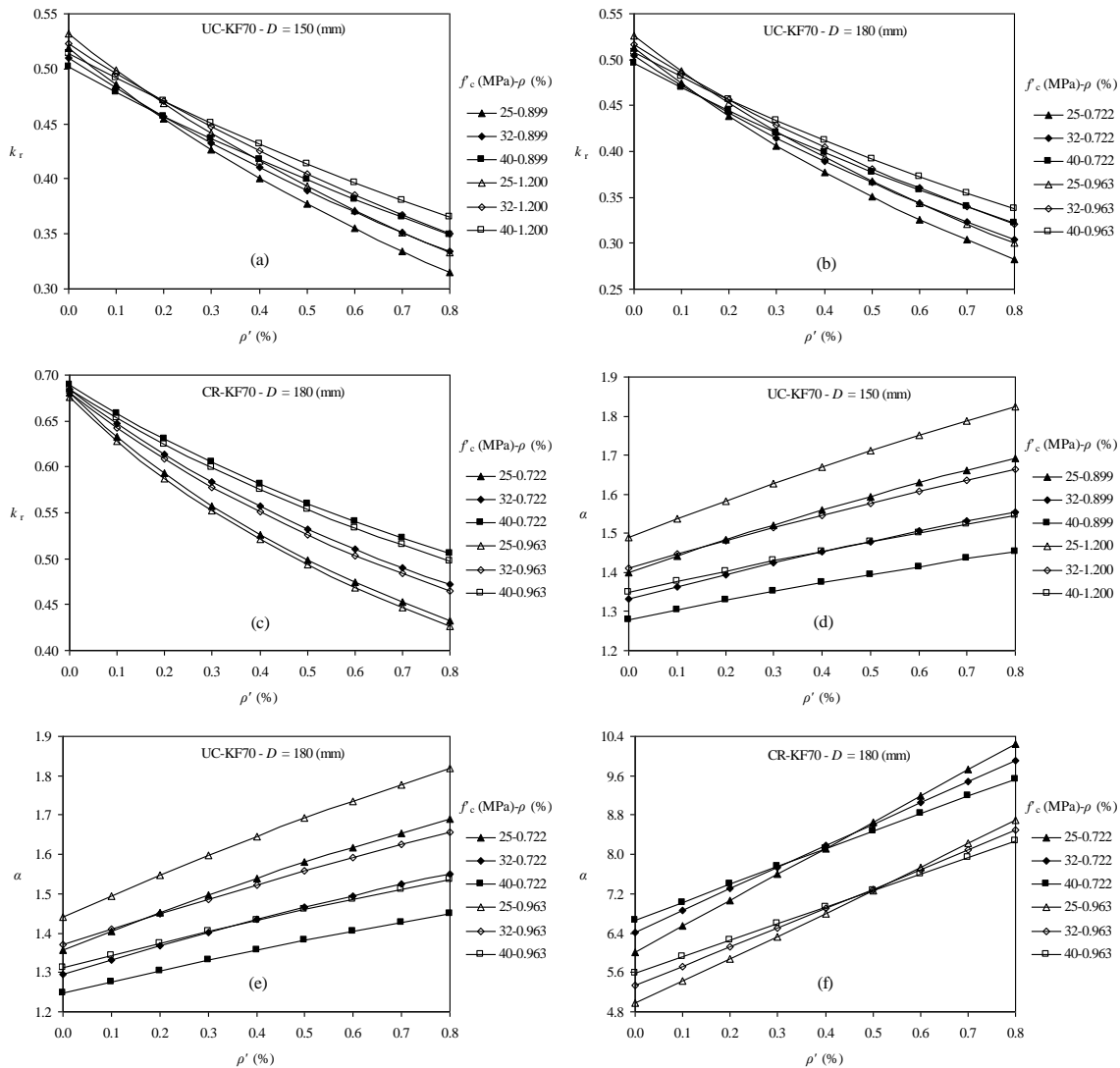


Figure 3. Values of k_r and α for uncracked and cracked KF70 sections ($D = 150$ and 180 mm).

Worked Examples

Two examples are solved here to show how the time-dependent deflection can be calculated by using the graphs of Fig. 3.

Example-1: The time-dependent deflections of two identical slabs 2LT-70-3 and 3LT-70-3 tested by Gholamhoseini et al. (2012b) are to be calculated. Each slab was simply-supported over a span of 3100 mm, with a 1200 mm wide and 150 mm thick cross-section and with 0.75 mm thick KF70 steel decking. Both slabs contained no reinforcement (other than the external steel decking). The centre to centre distance between the supports (one hinge and one roller) was 3100 mm. Each slab was placed onto its supports at age 7 days and carried only its self-weight (3.60 kN/m) until age 64 days. At age 64 days, an additional uniformly distributed superimposed sustained load of 4.08 kN/m was applied to each slab and remained in place until the end of the test period at age 247 days. Both slabs remained uncracked throughout the test period.

The required data are:

$E_c = 30725 \text{ MPa}$, $f'_c = 28 \text{ MPa}$, $A_{sd} = 1320 \text{ mm}^2$, $y_{sd} = 27.7 \text{ mm}$, $A_c = 148.8 \times 10^3 \text{ mm}^2$ (gross area of concrete cross-section), $I_{un-cr} = 278 \times 10^6 \text{ mm}^4$ (second moment of area of the transformed uncracked slab), $d = 122.3 \text{ mm}$, $\rho = 0.00899$, $k_4 = 0.65$, $k_5 = 1.0$ and $\phi_{cc,b} = 3.86$

Solution: The average concrete thickness and hypothetical thickness are:

$$t_{ave} = A_c / b = 148.8 \times 10^3 / 1200 = 124.0 \text{ mm} \quad t_h = 50 + \frac{t_{ave}}{2} = 112.0 \text{ mm}$$

The shrinkage strain is determined in accordance with AS 3600-2009 as:

$$\varepsilon_{sh}(247,7) = -530 \times 10^{-6}$$

For loading at ages 7 days and 64 days, the creep coefficient is determined in accordance with AS 3600-2009 as:

$$\phi(247,7) = 5.43, \quad \phi(247,64) = 3.14$$

The instantaneous deflections at the time of placing the slabs on the supports at age 7 days under the self-weight loading and at age 64 days caused by application of the superimposed sustained load of 4.08 kN/m are:

$$(\Delta_{i.sus})_7 = \frac{5}{384} \frac{w_{sw} L^4}{E_c I_{un-cr}} = \frac{5}{384} \frac{3.60 \times 3100^4}{30725 \times 278 \times 10^6} = 0.51 \text{ mm}, \quad (\Delta_{i.sus})_{64} = \frac{5}{384} \frac{4.08 \times 3100^4}{30725 \times 278 \times 10^6} = 0.57 \text{ mm}$$

From Fig. 3(a), the shrinkage modification factor for uncracked slab is $k_r = 0.52$ and the shrinkage-induced curvature is obtained from Eq. 1 as:

$$\kappa_{sh.uc} = \frac{0.52 \times 530 \times 10^{-6}}{150} = 1.84 \times 10^{-6} \text{ mm}^{-1}$$

And the shrinkage-induced deflection Δ_{sh} at age 247 days is:

$$\Delta_{sh} = \frac{\kappa_{sh.uc} L^2}{8} = \frac{1.84 \times 10^{-6} \times 3100^2}{8} = 2.21 \text{ mm}$$

From Fig. 3(d), the creep modification factor is $\alpha = 1.37$ and, since the slabs are uncracked between age 7 days and 247 days, the creep-induced deflection Δ_{creep} may be simply calculated as:

$$\Delta_{creep} = \frac{\phi(247,7)}{\alpha} (\Delta_{i.sus})_7 + \frac{\phi(247,64)}{\alpha} (\Delta_{i.sus})_{64} = \frac{5.43}{1.37} \times 0.51 + \frac{3.14}{1.37} \times 0.57 = 3.33 \text{ mm}$$

Therefore, the time-dependent change in deflection between first loading (7 days) and age 247 days is:

$$\Delta_{time} = (\Delta_{i.sus})_{64} + \Delta_{sh} + \Delta_{creep} = 0.57 + 2.21 + 3.33 = 6.11 \text{ mm}$$

This compares well with the measured deflection of the two slabs (i.e. 6.72 mm and 5.84 mm) and the value of 6.04 mm calculated in a numerical analysis by Gholamhoseini et al. (2012b) using the age-adjusted effective modulus method (AEMM) to model the non-linear time-dependent behaviour of concrete. Similar calculations were carried out at regular intervals throughout the duration of the test and the results are presented in Fig. 4, showing excellent agreement with both the test and analytical outcomes.

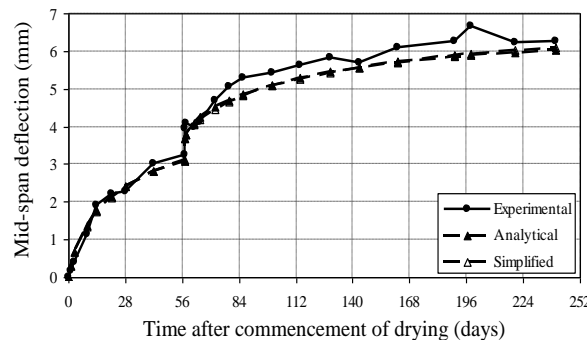


Figure 4. Mid-span deflection versus time curves in Example 1.

Example-2: The final total deflection of a simply-supported, 180 mm thick, one-way slab with 1 mm thick KF70 decking is to be calculated. The span of the slab is 4800 mm. The slab props are removed at age 7 days and the slab carries its self-weight (3.8 kN/m^2) and two line loads of $P = 8.0 \text{ kN/m}$ applied to the slab, as shown in Fig. 5a. The loads are assumed to remain permanently in place until $t = 10^4$ days. The bending moment diagram due to the sustained service load is shown in Fig. 5b. The cracking moment for the slab at the time of loading is $M_{cr} = 13.0 \text{ kNm/m}$. The slab contains 12 mm diameter bars at 200 mm centres located

30 mm from the top surface of the slab throughout the span ($d' = 150$ mm). The slab is located in a near-coastal environment in Melbourne.

Take $f'_c = 32$ MPa, $E_c = 30100$ MPa, $A_{sc} = 550$ mm²/m, $\rho' = A_{sc} / bd' = 0.0037$, $A_{sd} = 1467$ mm²/m, $y_{sd} = 27.7$ mm, $d = 152.3$ mm, $\rho = A_{sd} / bd = 0.00963$, $w_{sw} = 3.8$ kPa (slab self-weight), $A_c = 154 \times 10^3$ mm²/m, $I_{un-cr} = 413 \times 10^6$ mm⁴/m, $I_{cr} = 147 \times 10^6$ mm⁴/m (second moment of area of the transformed cracked cross-section).

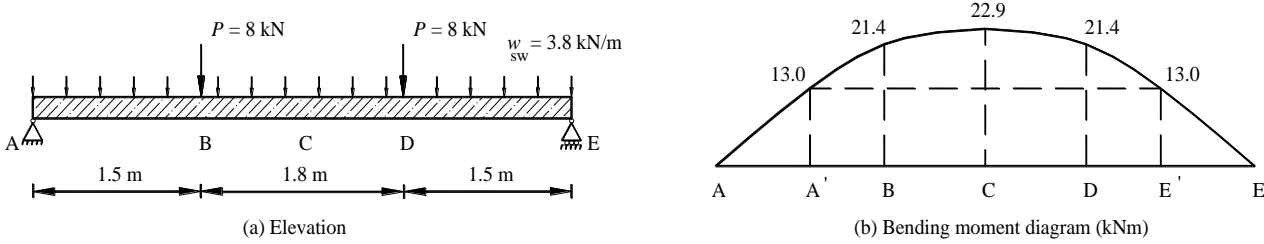


Figure 5. Loading configuration and bending moment diagram (Example 2).

Solution: The average concrete thickness is $t_{ave} = A_c / b = 154$ mm, and from Eq. 3, the hypothetical thickness is $t_h = 127$ mm. The final shrinkage strain is determined in accordance with AS 3600-2009 as $\epsilon_{sh}(10^4, 7) = 522 \times 10^{-6}$ and, for loading at ages 7 days, the final creep coefficient is determined in accordance with AS 3600-2009 as $\varphi(10^4, 7) = 4.23$.

From Figs. 3(b) and 3(c), the shrinkage modification factors for the uncracked and the cracked slab are $k_r = 0.41$ and $k_r = 0.56$, respectively. From Eq. 1, the final shrinkage-induced curvature on the uncracked and the cracked slab section are $\kappa_{sh,un-cr} = 1.19 \times 10^{-6}$ mm⁻¹ and $\kappa_{sh,cr} = 1.62 \times 10^{-6}$ mm⁻¹, respectively. From Fig. 3(e) and 3(f), the creep modification factors for uncracked and the cracked slab are $\alpha = 1.51$ and $\alpha = 6.78$, respectively.

The final curvature is now calculated at selected points along the span, notably at A, A', B, C, D, E' and E (as shown in Fig. 5).

At A (and E): At each support, $M_s^* = 0$, and the slab is uncracked. Thus, $\kappa = \kappa_{sh,un-cr} = 1.19 \times 10^{-6}$ mm⁻¹.

At A' (and E'): At the point between A and B (and between D and E), where $M_s^* = M_{cr} = 13.0$ kNm/m (i.e. at 0.837 m from each support), for long-term calculations $\beta = 0.5$, and from Eq. (7), $\zeta = 0.5$. The instantaneous curvatures on the uncracked and cracked sections are $\kappa_{i,un-cr} = M_s^* / E_c I_{un-cr} = 1.05 \times 10^{-6}$ mm⁻¹ and $\kappa_{i,cr} = M_s^* / E_c I_{cr} = 2.94 \times 10^{-6}$ mm⁻¹, respectively. From Eq. 2, the creep-induced curvature on the uncracked and cracked sections are $\kappa_{creep,un-cr} = \kappa_{i,un-cr} (\varphi(10^4, 7) / \alpha) = 2.94 \times 10^{-6}$ mm⁻¹ and $\kappa_{creep,cr} = \kappa_{i,cr} (\varphi(10^4, 7) / \alpha) = 1.83 \times 10^{-6}$ mm⁻¹, respectively. Therefore, the final curvatures on the uncracked and cracked sections are $\kappa_{un-cr} = \kappa_{i,un-cr} + \kappa_{creep,un-cr} + \kappa_{sh,un-cr} = 5.18 \times 10^{-6}$ mm⁻¹ and $\kappa_{cr} = \kappa_{i,cr} + \kappa_{creep,cr} + \kappa_{sh,cr} = 6.39 \times 10^{-6}$ mm⁻¹, respectively. The final curvature is obtained from Eq. 6, $\kappa = 5.79 \times 10^{-6}$ mm⁻¹.

Similarly at **B (and D):** $M_s^* = 21.4$ kNm/m, $\zeta = 0.82$, $\kappa_{i,un-cr} = 1.72 \times 10^{-6}$ mm⁻¹, $\kappa_{i,cr} = 4.84 \times 10^{-6}$ mm⁻¹, $\kappa_{creep,un-cr} = 4.82 \times 10^{-6}$ mm⁻¹, $\kappa_{creep,cr} = 3.02 \times 10^{-6}$ mm⁻¹, $\kappa_{un-cr} = 7.73 \times 10^{-6}$ mm⁻¹, $\kappa_{cr} = 9.48 \times 10^{-6}$ mm⁻¹ and $\kappa = 9.17 \times 10^{-6}$ mm⁻¹.

Similarly at **C:** $M_s^* = 22.9$ kNm/m, $\zeta = 0.84$, $\kappa_{i,un-cr} = 1.84 \times 10^{-6}$ mm⁻¹, $\kappa_{i,cr} = 5.18 \times 10^{-6}$ mm⁻¹, $\kappa_{creep,un-cr} = 5.15 \times 10^{-6}$ mm⁻¹, $\kappa_{creep,cr} = 3.23 \times 10^{-6}$ mm⁻¹, $\kappa_{un-cr} = 8.18 \times 10^{-6}$ mm⁻¹, $\kappa_{cr} = 10.03 \times 10^{-6}$ mm⁻¹ and $\kappa = 9.73 \times 10^{-6}$ mm⁻¹.

Deflection: The final mid-span deflection is readily calculated by double integration of the curvature diagram (shown in Fig. 6) or using, for example, the conjugate beam method of analysis and is determined as:

$$\Delta_{final} = 24.03 \text{ mm}$$

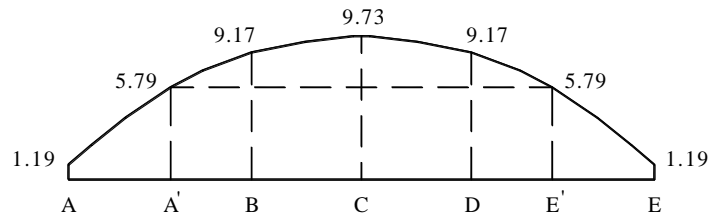


Figure 6. Final curvature diagram for Example 2, $\kappa \times 10^{-6} \text{ (mm}^{-1}\text{)}$.

Concluding Remarks

The long-term behaviour of composite concrete slabs under sustained service loads has been discussed. In particular, the time-dependent effects of creep and shrinkage have been outlined and graphs have been presented to show how to consider these effects using a simplified calculating procedure suitable for routine use in structural design. The graphs were developed using a more sophisticated cross-sectional analysis presented by the authors in a previous paper (Gilbert et al., 2012). The use of the graphs is illustrated by two worked examples and the results are compared against experimental and numerical results. Good agreement is obtained between the calculated and measured deflections.

References

- British Standards Institution, 2004. *Eurocode 2: Design of Concrete Structures-Part 1-1: General Rules and Rules for Buildings. BS EN 1992-1-1*, European Committee for Standardization, Brussels, Belgium.
- Carrier, R.E., Pu, D.C., and Cady, P.D., 1975. Moisture Distribution in Concrete Bridge Decks and Pavements, *Durability of Concrete, SP-47, American Concrete Institute*, Farmington Hills, MI, USA, 169-192.
- Fielders Australia PL, 2008. *Specifying Fielders-KingFlor, Composite Steel Formwork System Design Manual*.
- Gholamhoseini, A., Gilbert, R.I., Bradford, M.A., and Chang, Z.T., 2012a. Long-term Deformation of Composite Concrete Slabs under Sustained Loading, *Proceedings of the ACMSM22 Conference*, Sydney, Australia.
- Gholamhoseini, A., Gilbert, R.I., Bradford, M.A., and Chang, Z.T., 2012b. Long-term Deformation of Composite Concrete Slabs, *Concrete in Australia*, 38, 25-32.
- Gholamhoseini, A., Gilbert, R.I., Bradford, M.A., and Chang Z.T., 2014a. Time-Dependent Deflection of Composite Concrete Slabs, *ACI Structural Journal*, 111 (4), 765-776.
- Gholamhoseini, A., Gilbert, R.I., and Bradford, M.A., 2014b. Time-Dependent Deflection of Composite Concrete Slabs: A Simplified Design Approach, *Australian Journal of Structural Engineering*, 15 (3), 287-298.
- Gilbert, R.I., Bradford, M.A., Gholamhoseini, A., and Chang, Z.T., 2012. Effects of Shrinkage on the Long-term Stresses and Deformations of Composite Concrete Slabs, *Engineering Structures*, 40, 9-19.
- Gilbert, R.I., 2001. Deflection Calculation and Control - Australian Code Amendments and Improvements, *ACI International SP 203, Code Provisions for Deflection Control in Concrete Structures*, Chapter 4, American Concrete Institute. Editors EG Nawy and A Scanlon, 45-78.
- Gilbert, R.I. and Ranzi, G., 2011. *Time-Dependent Behaviour of Concrete Structures*. Spon Press, London, UK.
- Ranzi, G., Ambrogi, L., Al-Deen, S., and Uy, B., 2012. Long-term Experiments of Post-tensioned Composite Slabs, *Proceedings of the 10th International Conference on Advances in Steel Concrete Composite and Hybrid Structures*, Singapore.
- Ranzi, G., Leoni, G., and Zandonini, R., 2013. State of the Art on the Time-Dependent Behaviour of Composite Steel-Concrete Structures, *Journal of Constructional Steel Research*, 80, 252-263.
- Standards Australia (AS 3600:2009), *Australian Standard for Concrete Structures*, Sydney, Australia.